

Figure S1

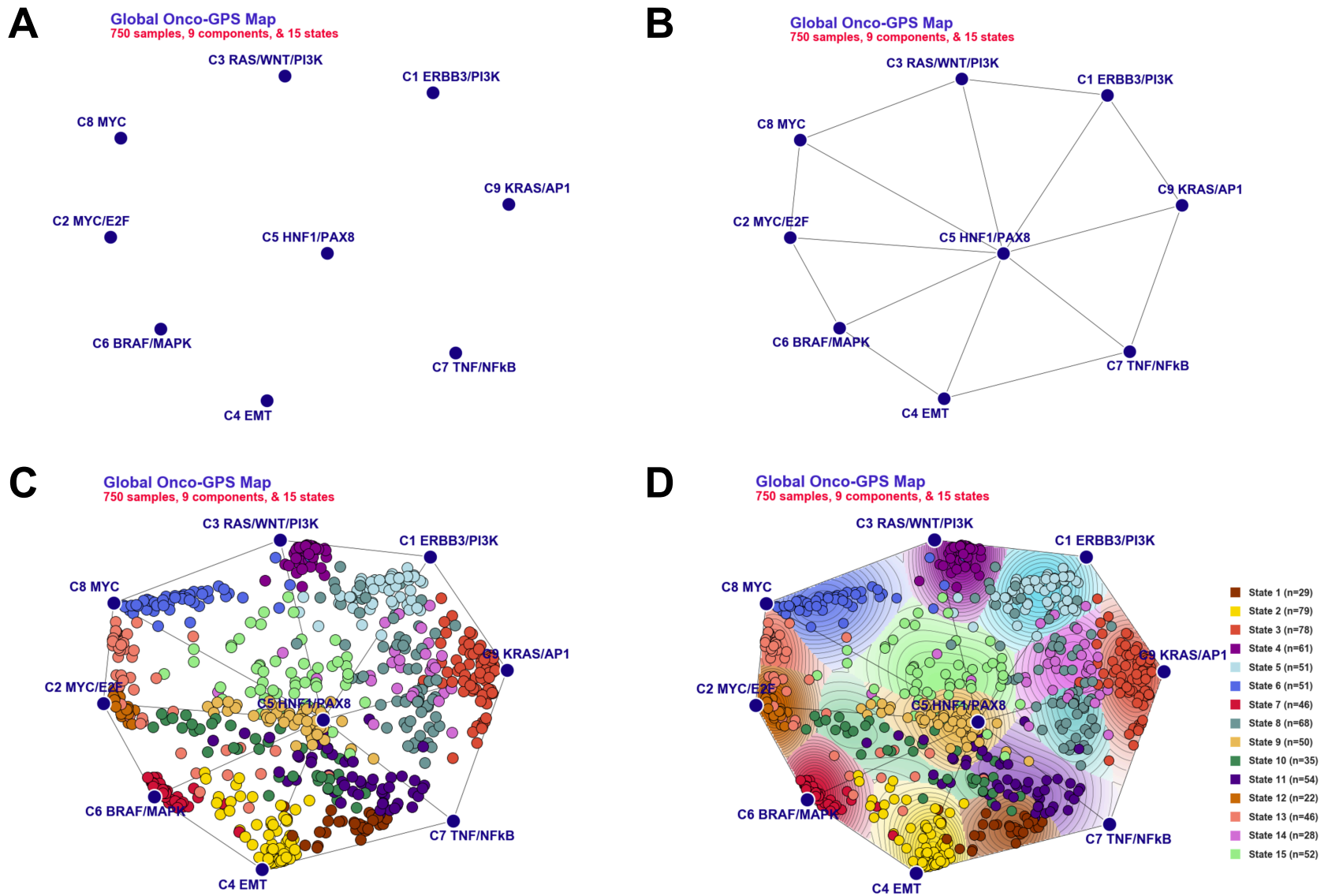


Figure S1. Related to main Figure 1 and 6. Generation of general (global) *Onco-GPS* layout: A) compute location of component nodes using a Sammon map projection, B) Add lines connecting component nodes using Delaunay triangulation, C) projection of individual cancer samples, and D) adding contours and color background to represent *Onco-GPS* states.

Figure S2

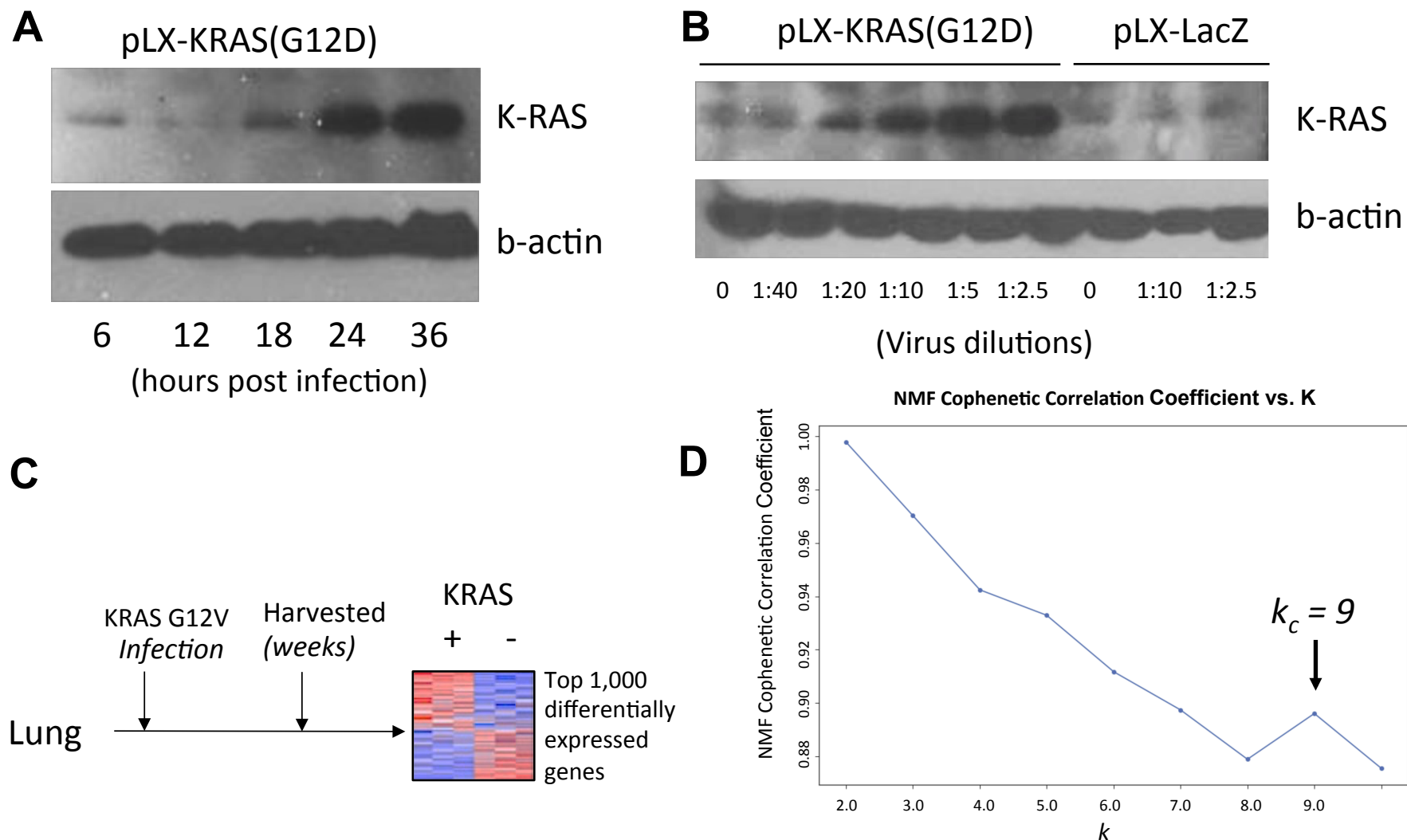


Figure S2. Related to main Figure 2 and 3. Optimization of **A**) dynamics and **B**) viral titers to induce KRAS activation; **C**) *KRAS* isogenic system generated from human lung cells. **D**) Stability of the *OncoGPS* NMF matrix decomposition. The graph shows the cophenetic coefficient as a function of component number. A peak in the cophenetic coefficient at $k = 9$ indicates a stable solution with 9 components.

Figure S3

Association of Component C3 with *KRAS* Mutation Status

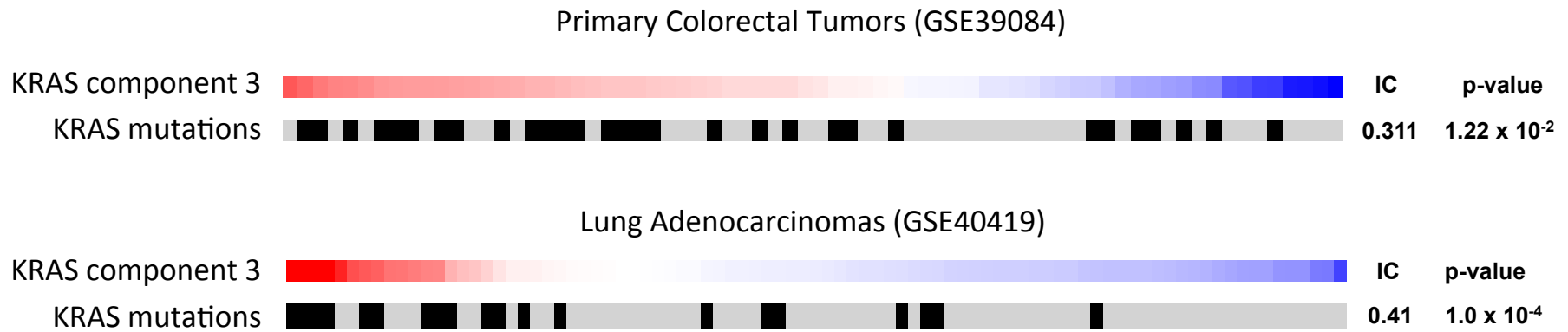


Figure S3. Related to main Figure 4. Association of component C3 with *KRAS* mutation status in primary colorectal (GEO dataset GSE39084) and lung adenocarcinomas (GEO dataset GSE40419).

Figure S4

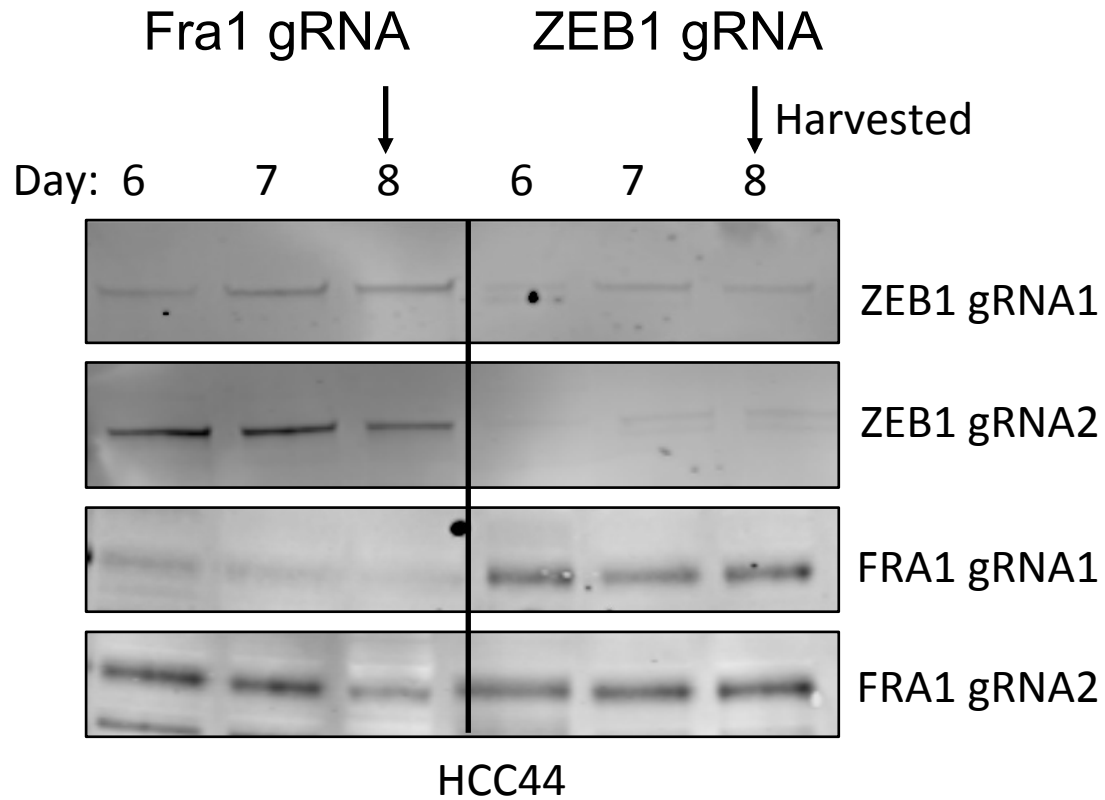


Figure S4. Related to main Figure 5. Confirmation of dynamics of protein decrease upon deletion of *FOSL1/FRA1* and *ZEB1* using gRNA CRISPR-CAS9 using immunoblotting. By day 8, the majority of proteins were suppressed and this day's sample was used for mRNA profiling.

Selected Features for KRAS Component C5

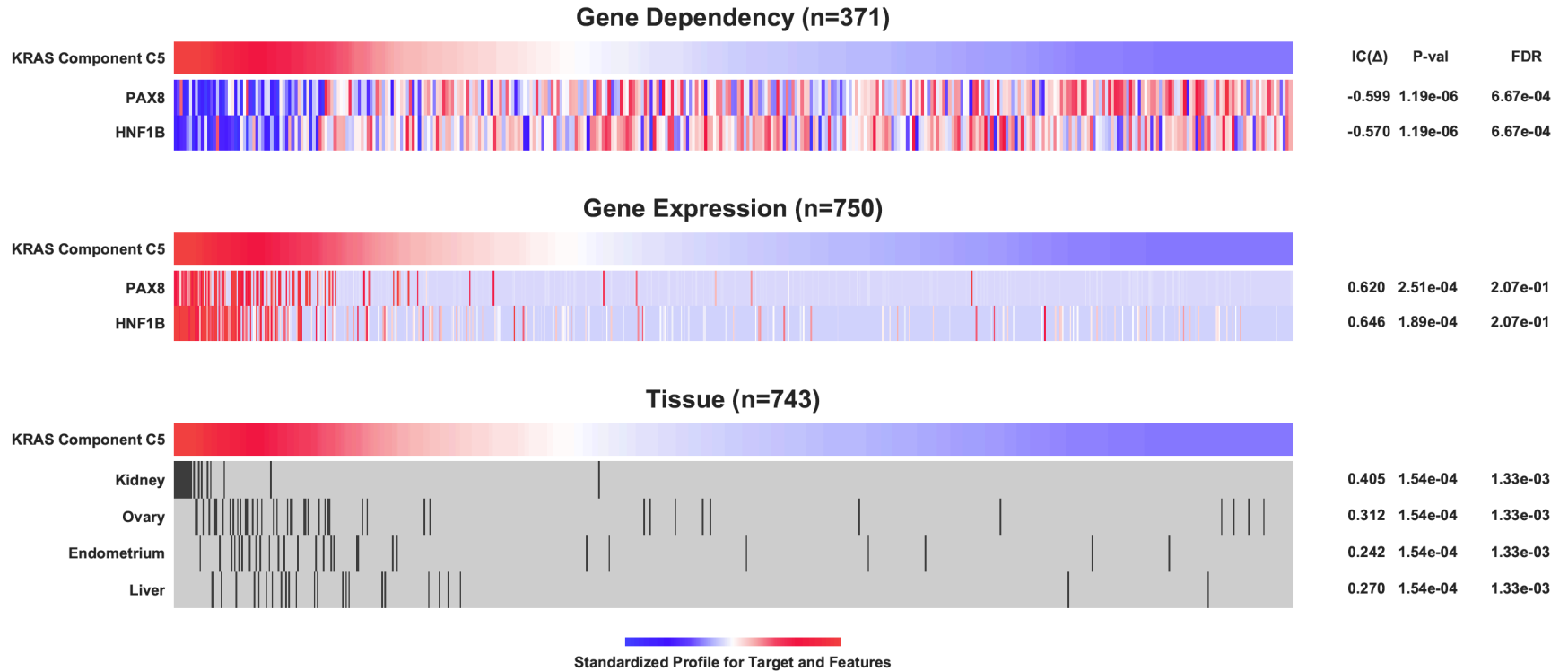


Figure S5. Related to main Figure 5. Selected features associated with component C5 in CCLE and Achilles datasets. Component C5 scores were associated with top features in Top) expression levels of PAX8 and HNF1B, Middle) PAX8 and HNF1B dependency from Achilles RNAi data, and Bottom) tissue type.

Figure S6

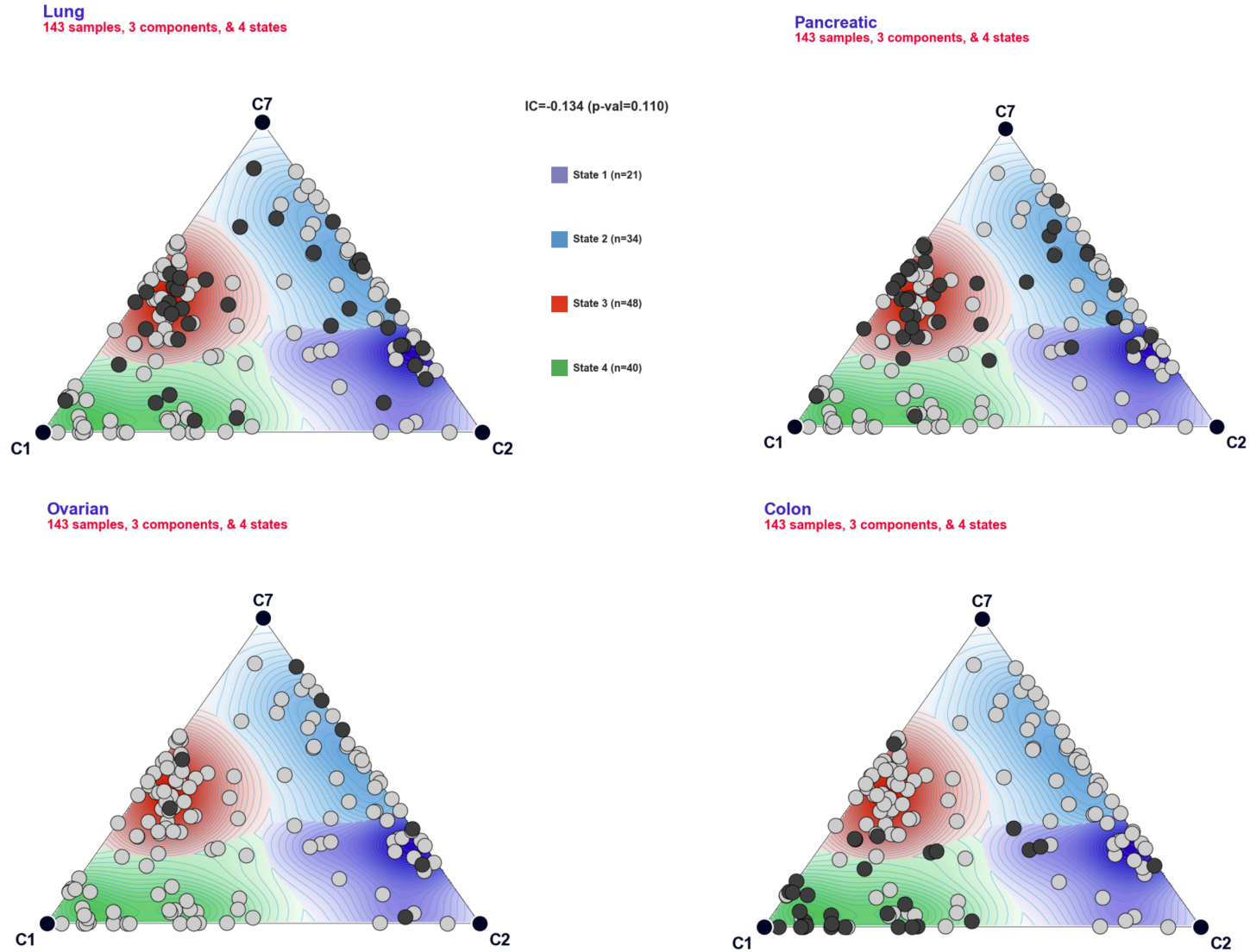


Figure S6. Related to main Figure 6. 4 Major tissue representations of KRAS mutant cancers across 4 cell states in the KRAS Onco-GPS map.

Figure S7

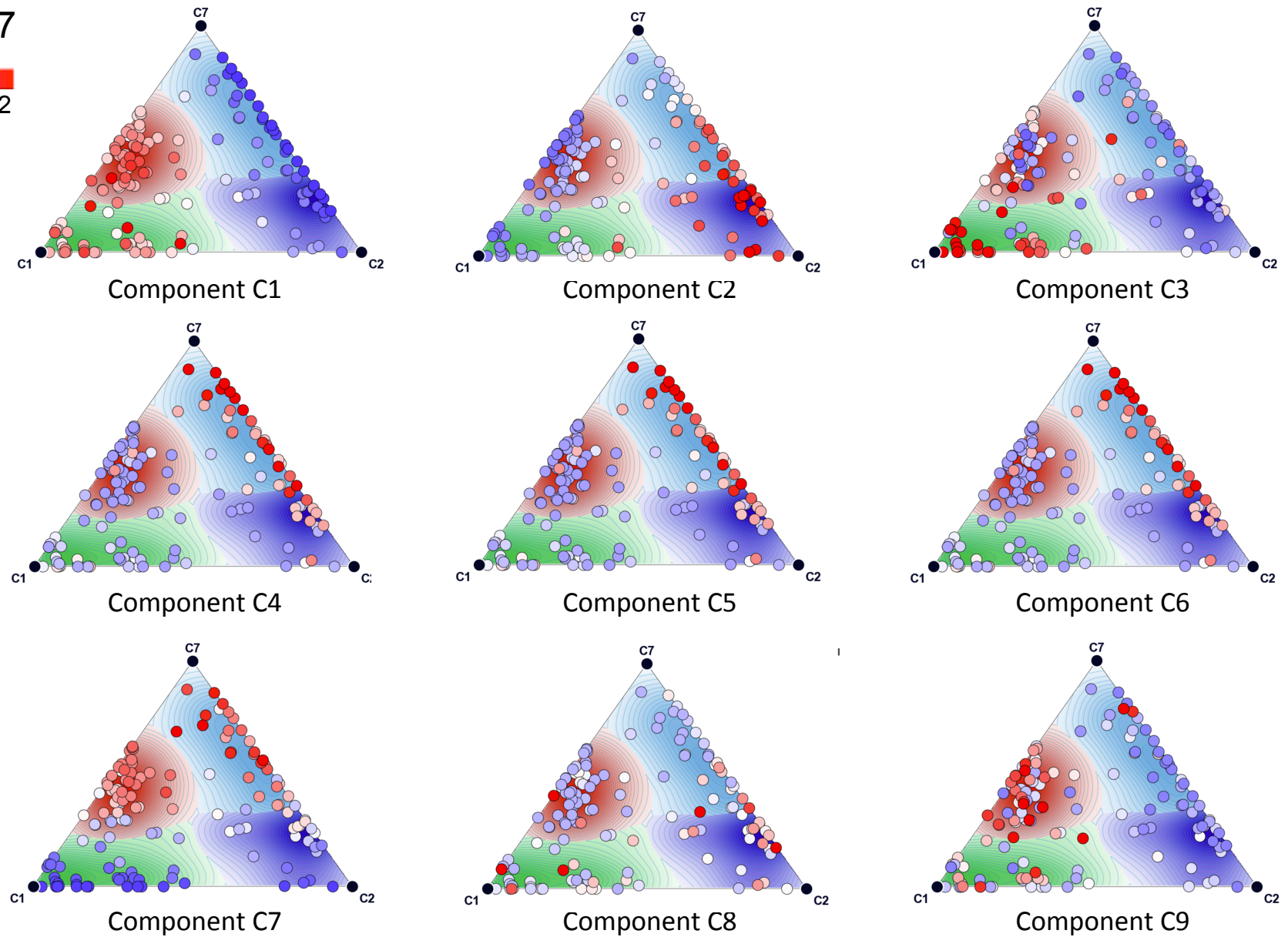


Figure S7. Related to main Figure 6. *Onco*-GPS maps defined by components C1-C7-C2 and the individual component scores projected as features (red-high, blue-low).

Figure S8

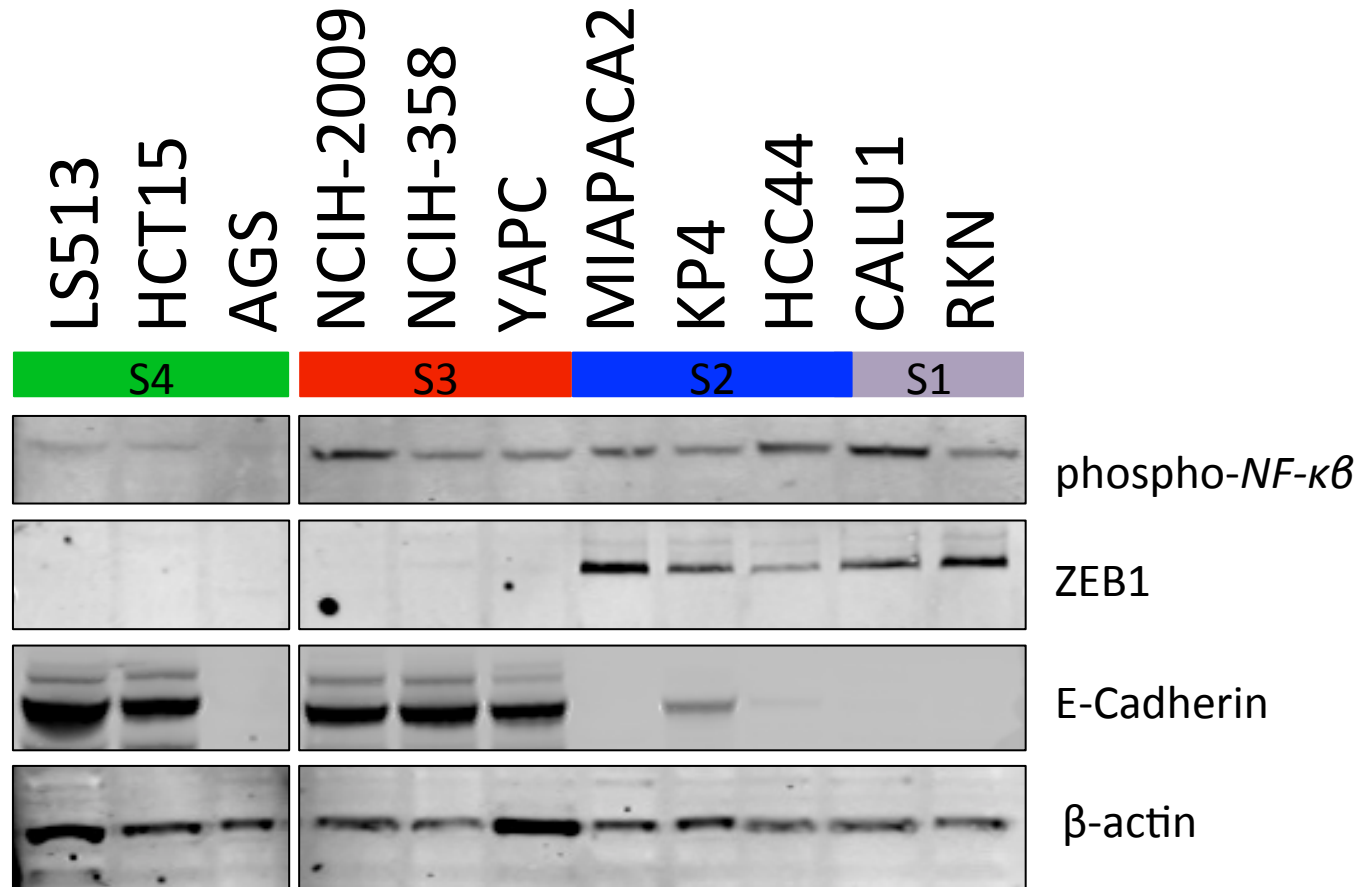
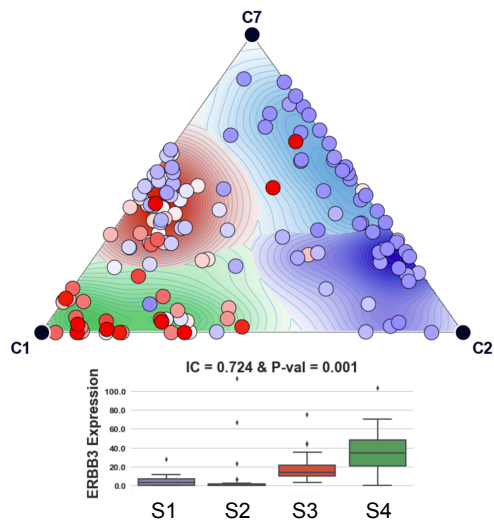


Figure S8. Related to main Figure 6. Immunoblots representing assessment of markers of epithelial-EMT state, and activation of NF-κB pathway across *KRAS* mutant cancers defined by *KRAS* *Onco*-GPS.

Figure S9

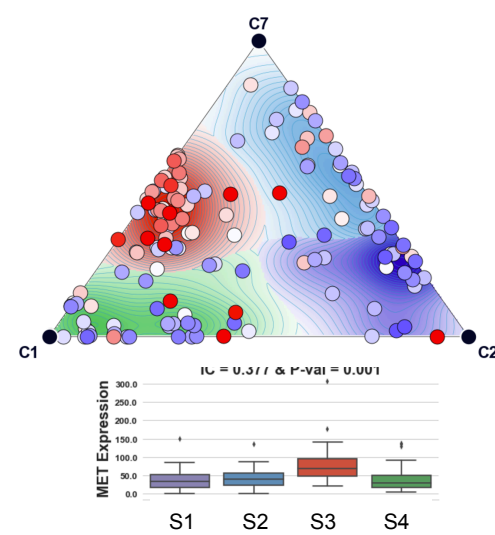
A

ERBB3 Expression
143 samples, 3 components, & 4 states



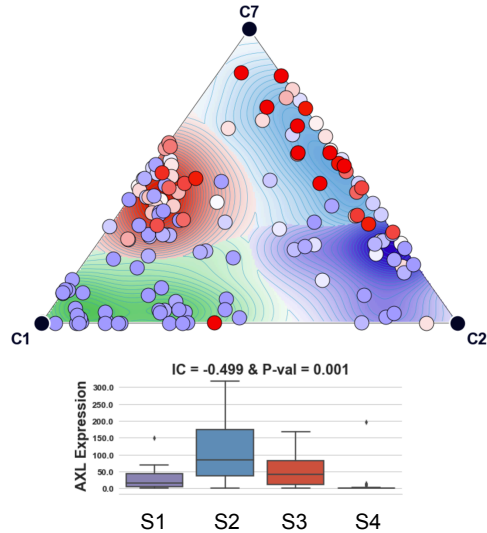
B

MET Expression
143 samples, 3 components, & 4 states



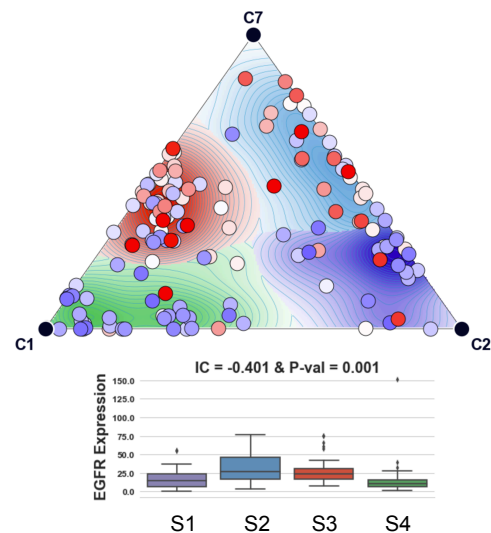
C

AXL Expression
143 samples, 3 components, & 4 states



D

EGFR Expression
143 samples, 3 components, & 4 states



E

CD274 (PD-L1) Expression
143 samples, 3 components, & 4 states

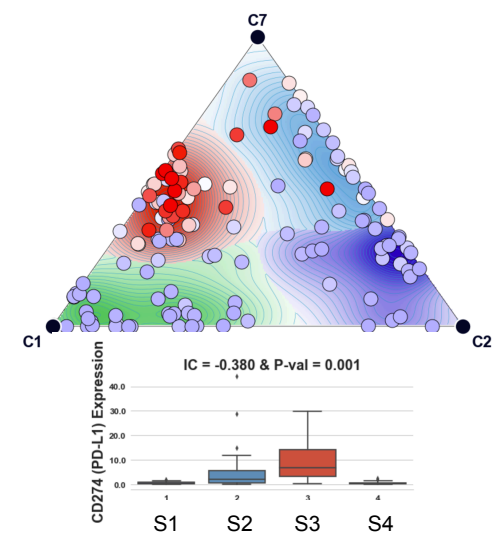


Figure S9. Related to main Figure. Onco-GPS maps and boxplots depicting transcript levels of RTKs: A) ERBB3, B) MET, C) AXL, D) EGFR and E) CD274 (PDL-1) in the S1-S4 KRAS mutant Onco-GPS states.

Figure S10

BRAF mutants

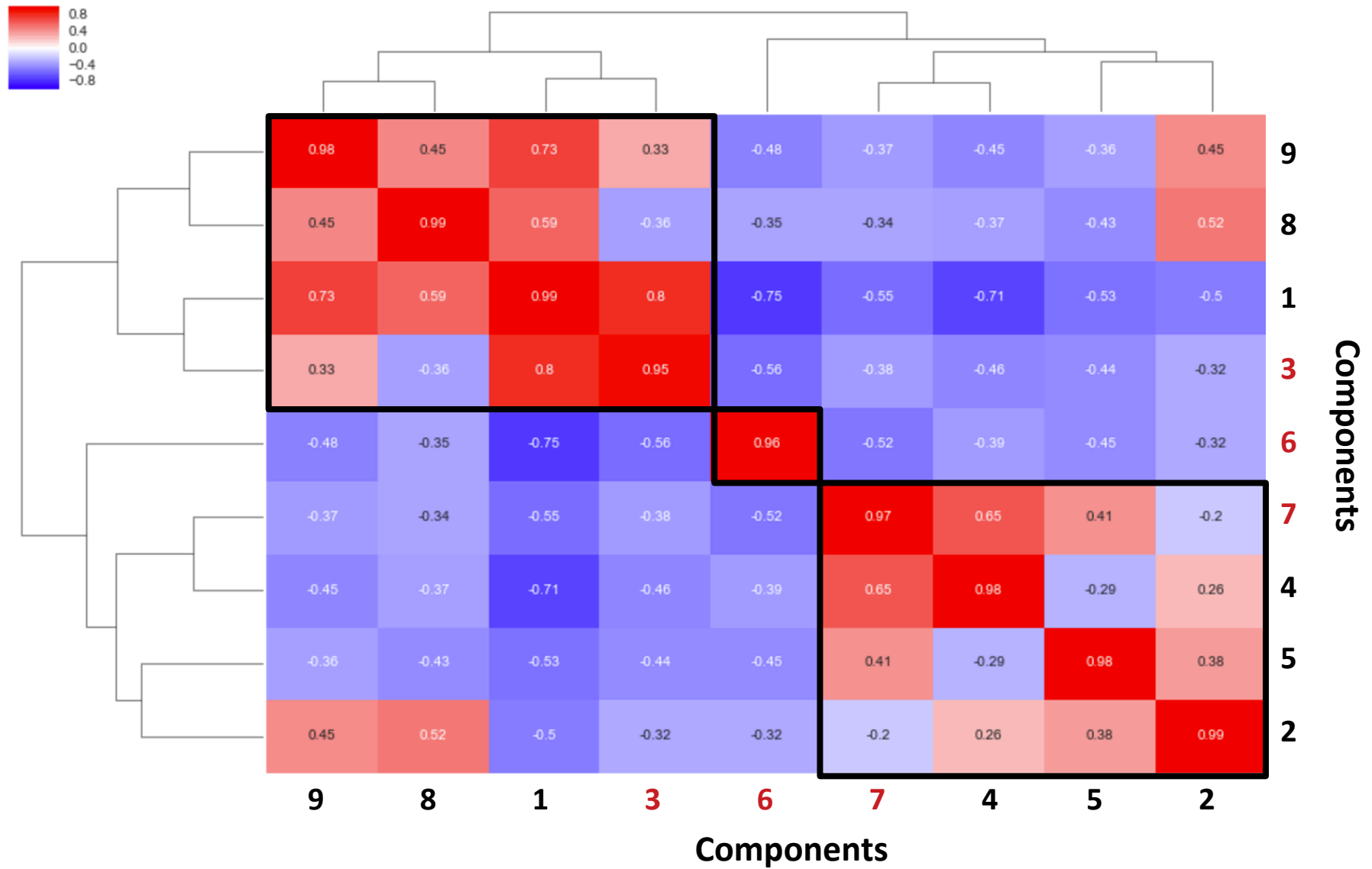


Figure S10. Related to main Figure 7. Association matrix of the 9 KRAS components (C1-C9) with each other according to the Information Coefficient (IC) in *BRAF* mutant samples. Components highlighted in red depict components that were chosen as representative components for subsequent analysis.

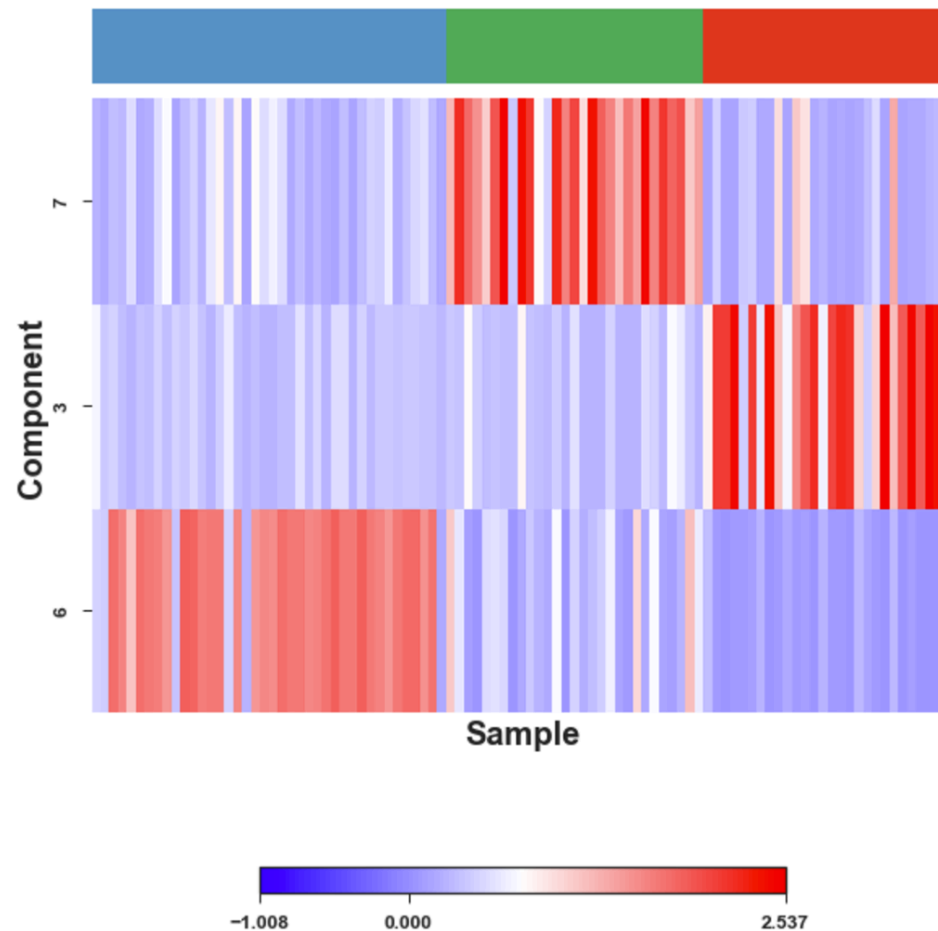
BRA F mutant samples classified by *Onco*-GPS state

Figure S11. Related to main Figure 7. Profile of components $C6$, $C7$ and $C3$ in the *BRAF* mutant samples. The color phenotypes correspond to the *Onco*-GPS states $S1$ - $S3$.

Figure S12

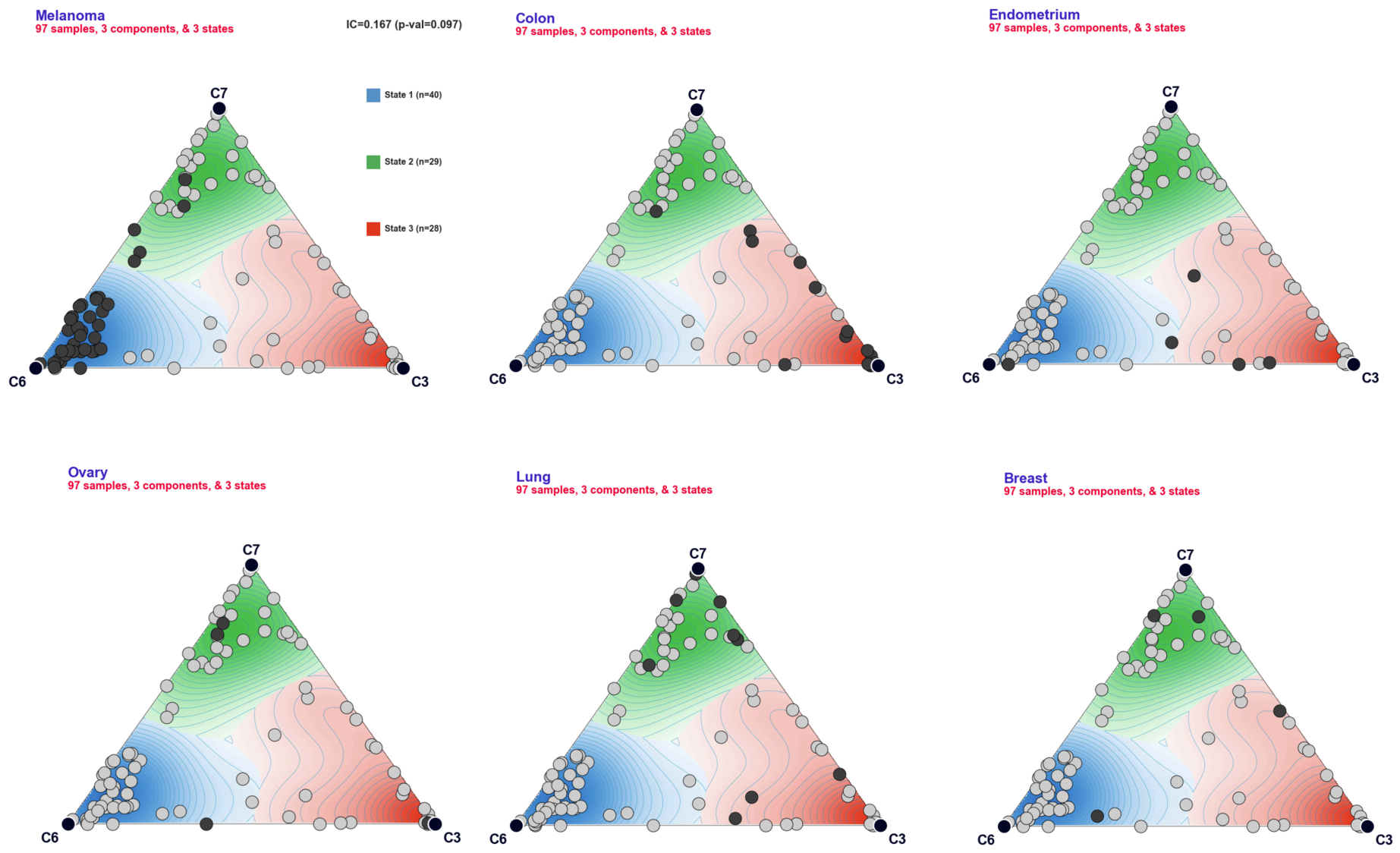
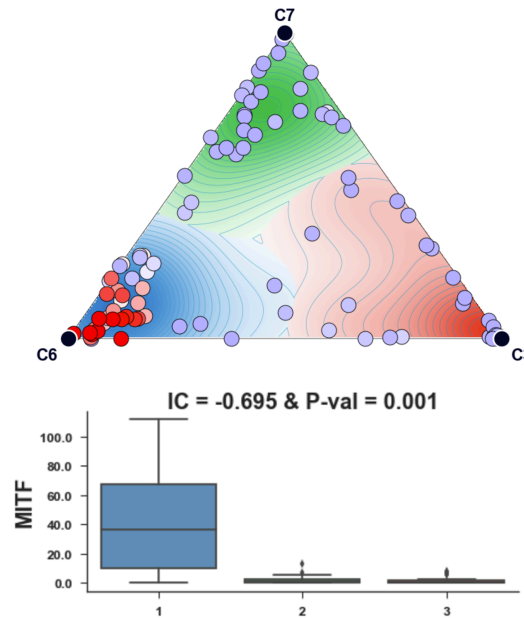


Figure S12. Related to main Figure 7. Tissue representation of BRAF mutant cancers across 3 cell states in the BRAF Onco-GPS map.

Figure S13

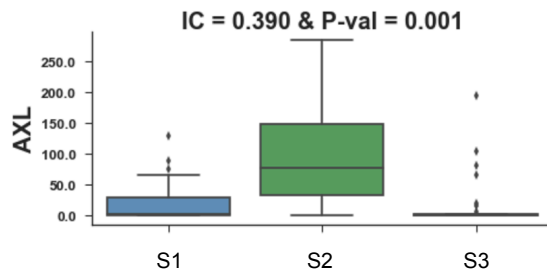
A

MITF Gene Expression



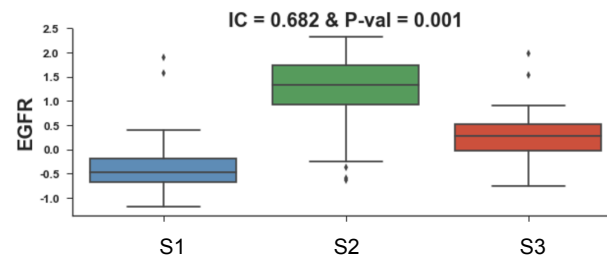
B

AXL Gene Expression



C

EGFR Expression (Protein)



D

SOX10 Gene Expression

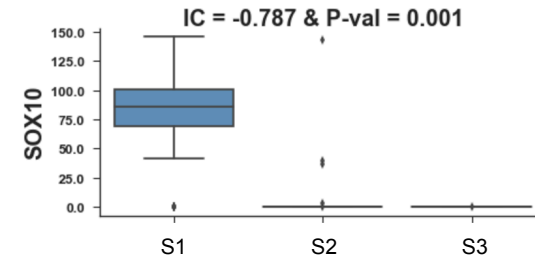


Figure S13. Related to main Figure 7. A) Gene expression of MITF across the *BRAF* mutants *Onco*-GPS states. Selected RTK's in the same *Onco*-GPS: B) AXL expression, C) EGFR (protein) and D) SOX10 expression.

Figure S14

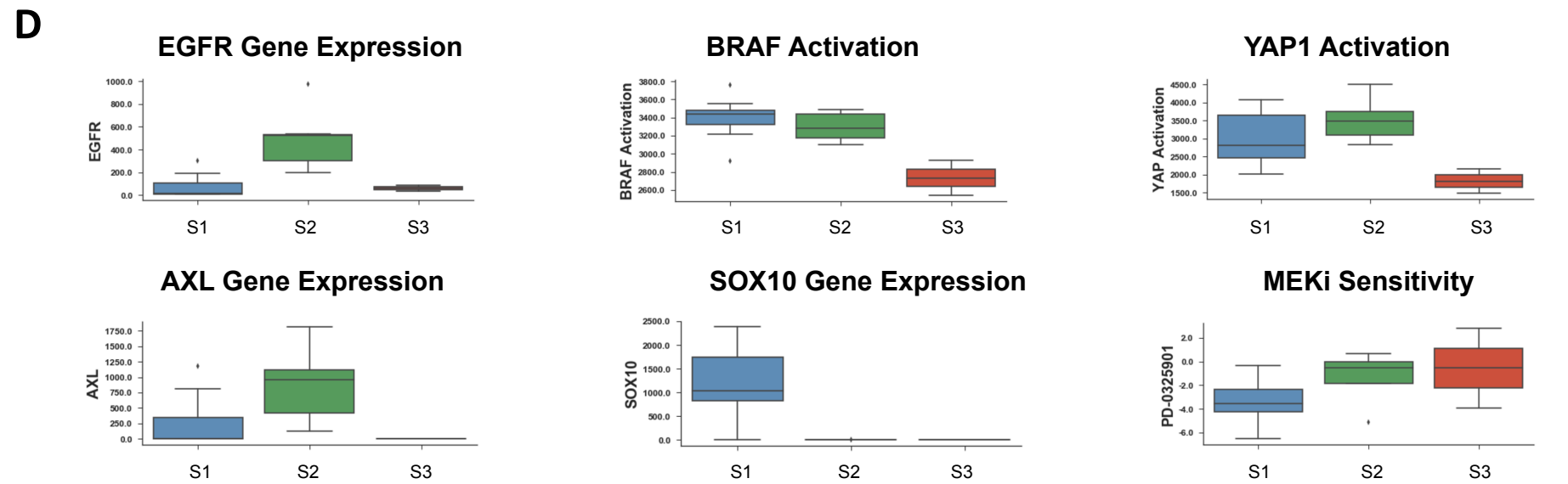
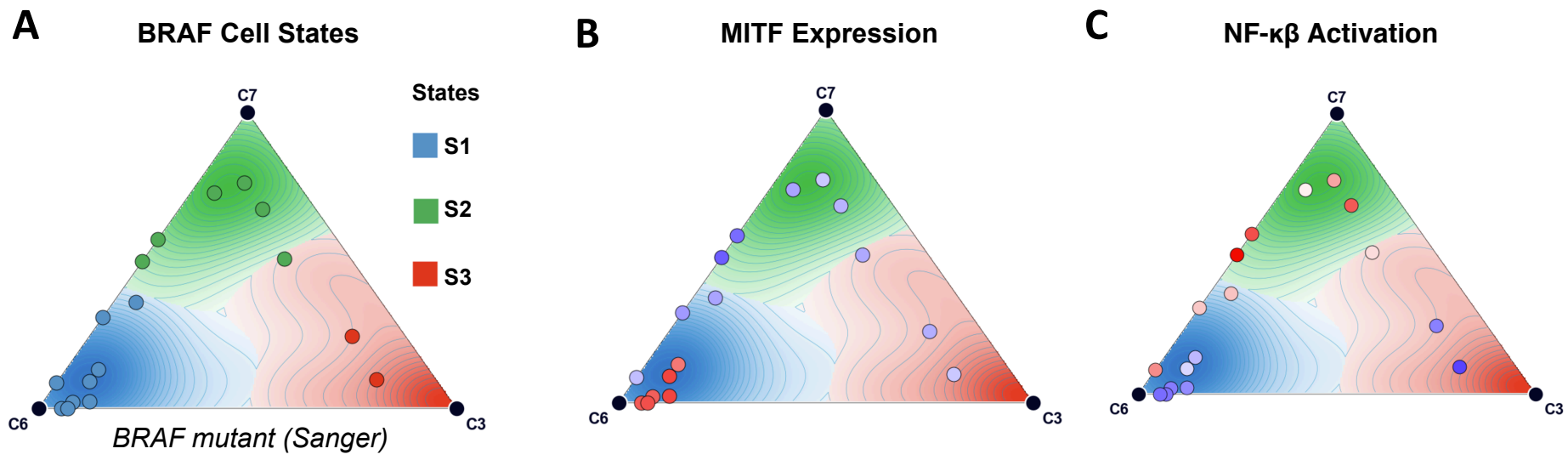
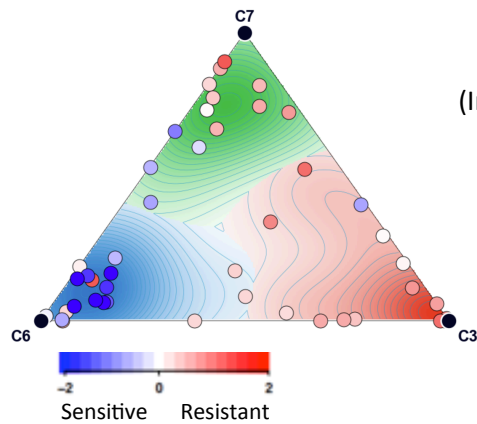


Figure S14. Related to main Figure 7. A) Projection of *BRAF* mutant non-overlapping samples in the Sanger dataset on top of the *BRAF Onco-GPS*. B) Expression of MITF, C) NF- κ B and D) selected RTK's display the same patterns as in the CCLE dataset.

Figure S15

A

Observed Sensitivity to BRAF Inhibitor (PLX-4720)

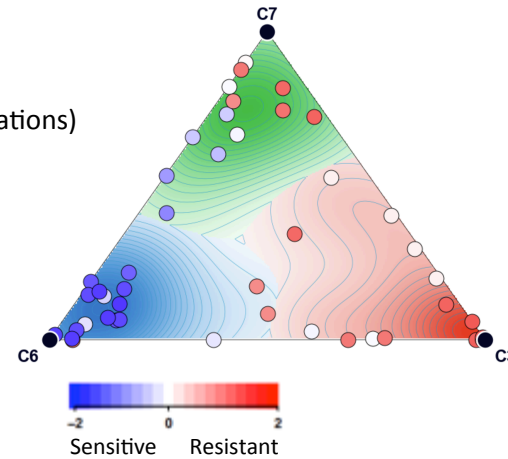


Train Probabilistic Model
(Inputs: C6 + C7 + NRAS/EGFR/KRAS mutations)

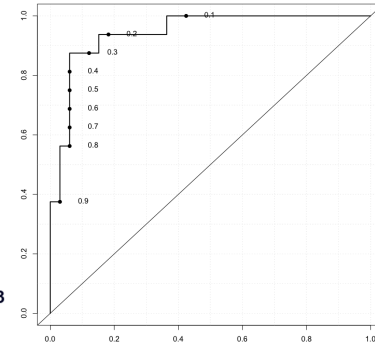


B

Predicted Sensitivity (Training/Model Fit)



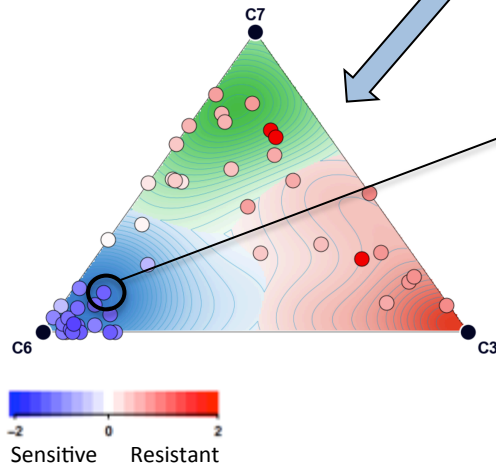
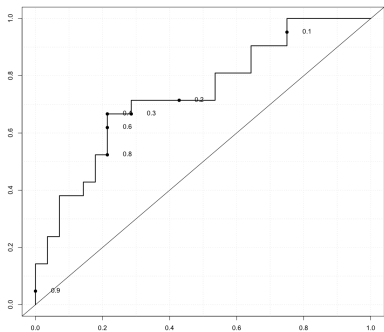
AUC ROC: 0.943
P-val: 8.17×10^{-9}



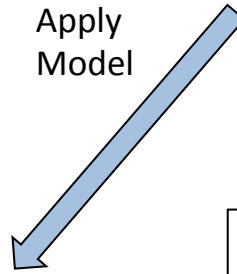
C

Predicted Sensitivity in Independent Test Dataset (Sanger)

AUC ROC: 0.735
P-val: 0.00237



Apply Model



D

Bayesian Nomogram for BRAF Inhibition Sensitivity

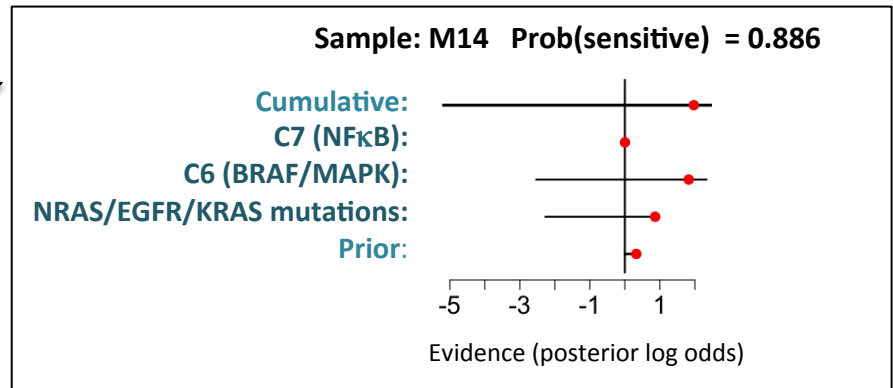


Figure S15. Related to main Figure 7. Probabilistic model for predicting BRAF inhibition: A) BRAF *Onco*-GPS showing observed sensitivity to the PLX-4720 BRAF inhibitor. B) Prediction/ROC curve (model fit) of samples in the training set. C) Prediction/ROC curve for samples in an independent test dataset (Sanger), and D) Bayesian nomogram showing an individual sample's prediction and the weight of evidence from each of the model inputs: C6, C7 and NRAS/EGFR/KRAS mutation status.

Figure S16

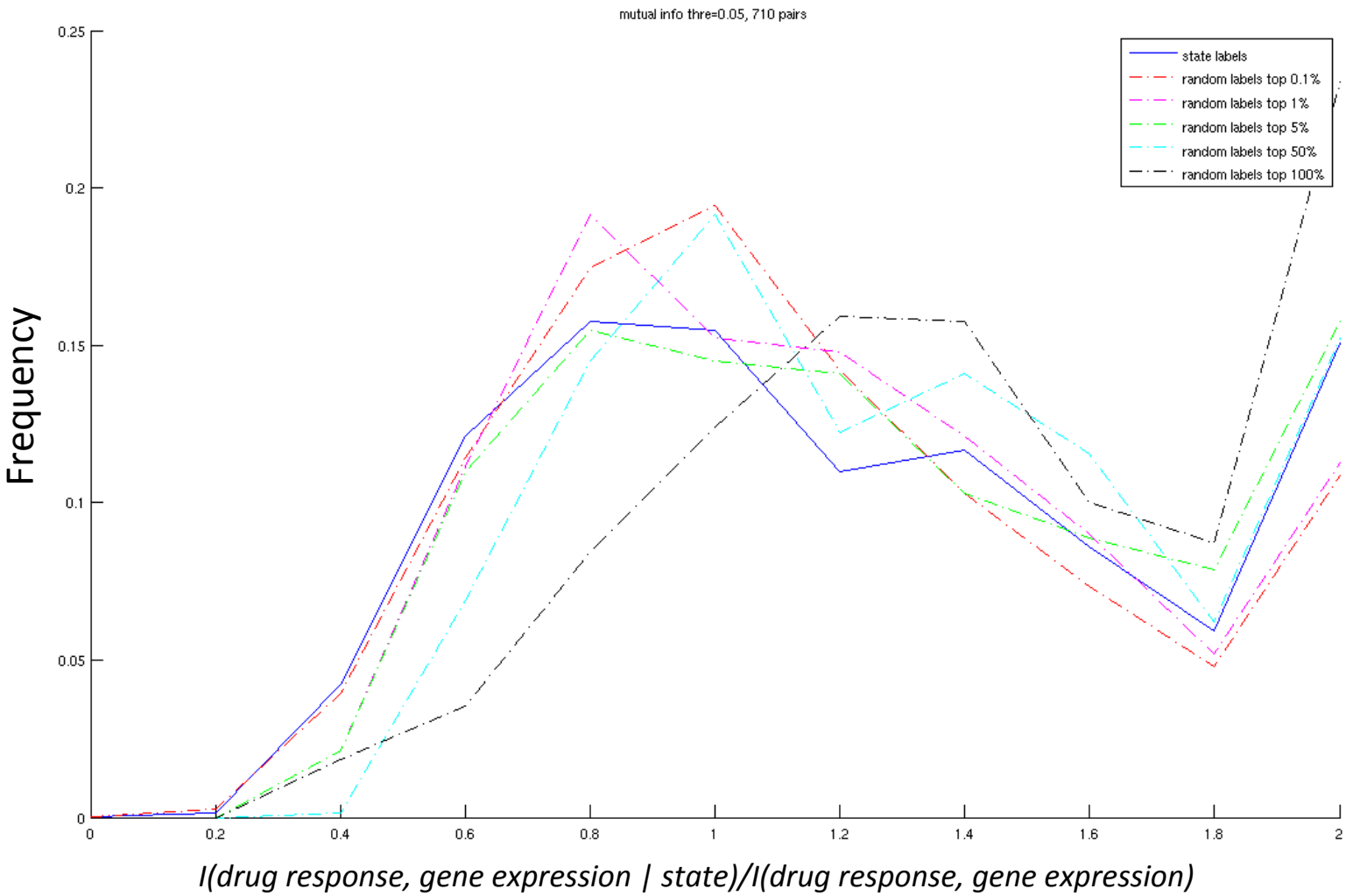
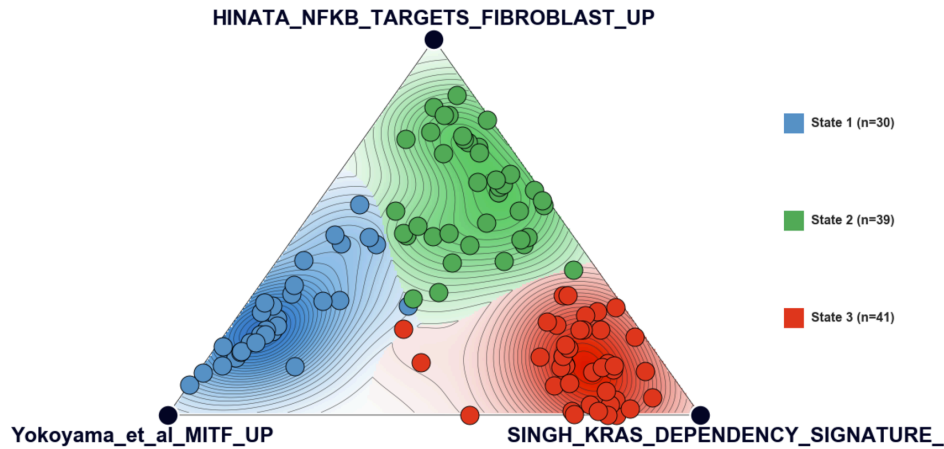


Figure S16. Related to main Figure 7. Observed and randomly permuted data distributions of *NCMI* scores for gene expression-drug response pairs whose mutual information is equal or greater than 0.05.

A

Pathway-Based (ssGSEA) *Onco*-GPS Map

BRAF Mutant *Onco*-GPS Map
110 samples, 3 components, & 3 states



B

Protein-Based (RPPA) *Onco*-GPS Map

BRAF Mutant *Onco*-GPS Map
106 samples, 3 components, & 3 states

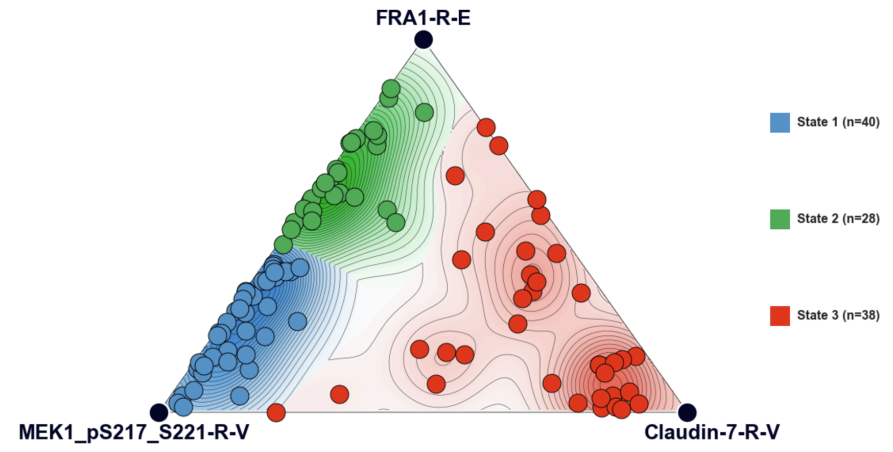


Figure S17. Related to main Figure 7. *BRAF* mutant *Onco*-GPS maps generated using as nodes: A) three single-sample GSEA scores of relevant gene sets, and B) three RPPA relevant protein profiles.